Published in final edited form as:
Clin Cancer Res. 2007 November 15; 13(22 Pt 1): 6769–6778. doi:10.1158/1078-0432.CCR-07-1536.

Preclinical Studies of Celastrol and Acetyl Isogambogic Acid in Melanoma

Sabiha Abbas, **Anindita Bhoumik**, **Russell Dahl**, **Stefan Vasile**, **Stan Krajewski**, **Nicholas D.P. Cosford**, and **Ze'ev A. Ronai**
Signal Transduction Program, Cancer Center, Burnham Institute for Medical Research, La Jolla, California

Abstract

Purpose—Sensitize melanomas to apoptosis and inhibit their growth and metastatic potential by compounds that mimic the activities of activating transcription factor 2 (ATF2)-driven peptides.

Experimental Design—Small-molecule chemical library consisting of 3,280 compounds was screened to identify compounds that elicit properties identified for ATF2 peptide, including (*a*) sensitization of melanoma cells to apoptosis, (*b*) inhibition of ATF2 transcriptional activity, (*c*) activation of c-Jun NH_2-terminal kinase (JNK) and c-Jun transcriptional activity, and (*d*) inhibition of melanoma growth and metastasis in mouse models.

Results—Two compounds, celastrol (CSL) and acetyl isogambogic acid, could, within a low micromolar range, efficiently elicit cell death inmelanoma cells. Both compounds efficiently inhibit ATF2 transcriptional activities, activate JNK, and increase c-Jun transcriptional activities. Similar to the ATF2 peptide, both compounds require JNK activity for their ability to inhibit melanoma cell viability. Derivatives of CSL were identified as potent inducers of cell death in mouse and human melanomas. CSL and a derivative (CA19) could also efficiently inhibit growth of human and mouse melanoma tumors and reduce the number of lung metastases in syngeneic and xenograft mouse models.

Conclusions—These studies show for the first time the effect of CSL and acetyl isogambogic acid on melanoma. These compounds elicit activities that resemble the well-characterized ATF2 peptide and may therefore offer new approaches for the treatment of this tumor type.

The growth and metastasis of melanoma as well as its notorious resistance to therapy present major obstacles to its treatment (1,2). A growing number of genetic and epigenetic changes in melanomas affect genes associated with melanocyte development and maintenance, cell cycle control, resistance to apoptosis, and angiogenic and metastatic capacity. Among the genetic changes commonly found in human melanomas are mutations in protein kinases of the mitogen-activated protein kinase (MAPK) family, indicating that signal transduction pathways have been largely modified in this tumor type (3,4). Specifically, the prevalence of activating mutations in *B-RAF* and *N-RAS* has been largely associated with the activation of downstream targets—MAPK/extracellular signal-regulated kinase (ERK) kinase and in many cases ERK-MAPK (5–7). Constitutive activation of these kinases results in corresponding up-regulation of their targets, including genes implicated in the development and maintenance of melanoma, such as *MITF*, *iNOS*, and *cyclin D1* (8–11).

Requests for reprints: Ze'ev A. Ronai, Signal Transduction Program, Burnham Institute for Medical Research, 10901 North Torrey Pines Road, La Jolla, CA 92037. Phone: 858-646-3185; Fax: 815-366-8003; ronai@burnham.org.

Note: Supplementary data for this article are available at Clinical Cancer Research Online (http://clincancerres.aacrjournals.org/).

In addition to changes in the MAPK signaling pathway, other pathways are deregulated in melanoma for reasons as yet unknown. For example, a growing fraction of melanomas is recognized as carrying an inactive form of PTEN, a protein phosphatase implicated in the regulation of *AKT* signaling pathways and their downstream mammalian target of rapamycin and p70S6 effectors (12,13). Up-regulation of protein kinase C and c-Jun NH_2-terminal kinase (JNK) has also been observed in melanoma (14–16). Other regulatory components that are modified in melanoma include cell cycle regulatory proteins, such as cyclin-dependent kinases (*CDKN2A*) *CDK2*, *p16/CDK/pRb*, and *cyclin D1* (17–19).

Modifications were also recorded in matrix metalloproteinase, proteases associated with tumor cell metastatic capacity (20–22), and chaperones such as HSP90 (23). The antiapoptotic proteins, such as Bcl2 and the transcription factors activating transcription factor (ATF) 1, AP1, and ATF2, also cooperate in conferring resistance to apoptosis and metastatic capacity on melanoma (24–26). The complexity of changes that take place in melanoma are further illustrated in the rewiring of key signal transduction pathways; for example, ERK causes up-regulation of c-Jun and JNK activity (27).

In earlier studies, we showed that the transcription factor ATF2 serves as a good marker and possible target for this tumor type (28–32). Analysis of 544 human melanomas using tissue arrays revealed that nuclear localization of ATF2 is associated with poor prognosis (28), thereby pointing to the possibility that constitutively active ATF2 may contribute to the development and progression of human melanomas. Consistent with this possibility, inhibition of ATF2 function by means of a 50-amino acid peptide derived from ATF2 sensitized melanoma to apoptosis (29) and inhibited growth and metastasis in mouse models (30,31). ATF2 peptides elicit such effects by virtue of their ability to inhibit ATF2 concomitant with an increase in JNK and consequently c-Jun activities (32). Given our understanding of the activities of the ATF2 peptide, we did a high-throughput screen to identify compounds that may mimic such activities. Characterization of two such compounds and newly generated derivatives in both *in vitro* and *in vivo* models suggests that they may have potential in the treatment of melanoma.

Materials and Methods

Cells

Mouse melanoma (SW1) and human melanoma (LU1205) cells were maintained in DMEM supplemented with 10% fetal bovine serum, L-glutamine, and antibiotics. The human melanoma cell lines MEWO and WM115 were maintained in RPMI 1640 supplemented with 10% fetal bovine serum and antibiotics. Primary mouse melanocytes were cultured in F-12 medium supplemented with 10% fetal bovine serum, antibiotics, isobutylmethylxanthine, bovine pituitary extract, and 12-*O*-tetradecanoylphorbol-13-acetate.

Constructs and inhibitors

An ATF2 peptide (amino acids 51–100) was cloned into HA-tagged pcDNA3 vector as described previously (30). 5xJun2tk-Luc (marker for ATF2 transcriptional activities), 5xTREtk-Luc (marker for AP1/c-Jun transcriptional activities), and 2xNF-κB-Luc were described previously (31). Pharmacologic inhibitor of JNK (SP600125) was purchased (EMD Biosciences) and added (5 μmol/L) to cultured cells as indicated in Results.

Transcriptional analysis

Transient transfection of different reporter constructs into melanoma cells was done using Lipofectamine Plus (Invitrogen). Luciferase activity was determined as described previously (32).

Mitochondrial activity and apoptosis

Cells were exposed to the chemicals for 12 to 48 has indicated in Results. To measure changes in mitochondrial activity reflective of general cell viability, the ATPLite assay was used according to the manufacturer's recommendations (Perkin-Elmer). Apoptosis analysis was done by flow cytometry of propidium iodide–stained cells. The percentage of cells to the left of the diploid G_0-G_1 peak, characteristic of hypodiploid cells that have partially lost DNA, was calculated as percentage of apoptotic cells (32). Analysis of changes in caspase-8 expression pattern was done using immunoblot analysis.

Chemical library screen

Cells (4,000) were seeded in a volume of 45 μL of medium per well using a Matrix WellMate bulk reagent dispenser. The cells were incubated for 24 h at 37°C in a humidified atmosphere containing 5% CO_2. Subsequently, 5 μL of 0.1 mmol/L compounds in 10% DMSO were added to each well (final compound concentration was 0.01 mmol/L in 1% DMSO) using a Beckman Coulter Biomek FX automated liquid handler. Two small-molecule chemical libraries were used in the study. These libraries were the Library of Pharmacologically Active Compounds (LOPAC^{1280} from Sigma-Aldrich) as well as the 2,000 compounds that comprise the Spectrum Collection from MicroSource Discovery Systems, Inc. Both of these libraries are composed of small molecules that are pharmacologically active. The spectrum collection contains not only 1,000 small-molecule compounds but also 1,000 pharmacologically active purified natural products. These libraries have previously been used for screening campaigns (33,34).

The treated cells were incubated for 24 h. After incubation, 25μL of ATPLite 1step (Perkin-Elmer) were added to each well. ATPLite uses a luciferase-based system to measure the relative quantity of ATP in a sample. It has been shown that ATP quantification can be used to measure cell proliferation and cytotoxicity (35). After the addition of ATPLite, the plates were read using the luminescence readout of a Molecular Devices Analyst HT multimode plate reader.

Compound synthesis

The celastrol (CSL) used for biological studies and to prepare amide and ester derivatives was obtained from Pay Pay Technologies as a dark red crystalline solid. The purity of this material was assessed by ^{1}H nuclear magnetic resonance and liquid chromatography-mass spectrometry and found to be >98%. For the synthesis of esters and amides, all reactions were conducted in standard glassware without special regard to atmosphere or moisture. Reagents and anhydrous solvents were commercially purchased and used without purification. The purification of target compounds was done with a Shimadzu Discovery preparative high-performance liquid chromatography system or an ISCO Companion 4× flash chromatography system. Product analysis and identity confirmation was done using a Shimadzu liquid chromatography-mass spectrometer and a Varian 300 MHz nuclear magnetic resonance spectometer.

General procedure for the synthesis of amide derivatives of CSL

CSL (22 mg, 0.048 mmol) in dimethylformamide (2 mL) was treated with Hunig's base (20 μL, 0.12 mmol), PyBOP (50 mg, 0.096 mmol), and the appropriate amine (0.05 mmol). After stirring for 20 h at room temperature, deionized water (15 mL) was added and the mixture was extracted by ethyl acetate twice. The combined organic layers were washed with brine, dried over $MgSO_4$, and evaporated via rotary evaporator to yield a dark oil. The crude product was purified by flash chromatography (ethyl acetate/hexanes) and lyophilized (Labconco lyophilizer) to give a dark orange to red solid with yields ranging from 57% to 82%.

General procedure for the synthesis of ester derivatives of CSL

CSL (22 mg, 0.048 mmol) in dimethylformamide (2 mL) was treated with $NaHCO_3$ (20 mg, 0.24 mmol) and the appropriate alkyl halide (0.05 mmol). After stirring for 36 h at room temperature, deionized water (15 mL) was added and the mixture was extracted by ethyl acetate twice. The combined organic layers were washed with brine, dried over $MgSO_4$, and evaporated via rotary evaporator to yield a dark red oil. The crude product was purified by flash chromatography (ethyl acetate/hexanes) and lyophilized (Labconco lyophilizer) to give a dark red solid with yields ranging from 72% to 95%.

Immunoblot analysis

Proteins prepared from cells at the indicated time points using radioimmunoprecipitation assay buffer and 75 μg were separated on SDS-PAGE followed by immunoblot analysis using the antibodies indicated. Antibodies used were as follows: anti-JNK (Santa Cruz Biotechnology), phosphorylated JNK (Promega), phoshorylated c-Jun (Cell Signaling), c-Jun (Santa Cruz Biotechnology), caspase-8 (BD Biosciences), AKT and phosphorylated AKT (BD Biosciences), and ERK and phosphorylated ERK (Cell Signaling).

Tumor growth and metastasis *in vivo*

SW1 melanoma cells are metastatic derivative of 1735p cells originally developed by Dr. M. Kripke (M. D. Anderson Cancer Center, Houston, TX; ref. 31). Green fluorescent protein (GFP)-expressing SW1 cells were established and used as a means to follow melanoma progression in real time (30). SW1-GFP cells were trypsinized, resuspended in PBS, and injected s.c. (1×10^6) into the lower flank of 6-to 7-week-old mice. When tumors reached a size of ~50 mm^3, the indicated compounds [100 μL of the vehicle—10% DMSO, 70% cremophor/ethanol (3:1), and 20% PBS and 1.0 mg/kg CSL or 0.5 mg/kg of the derivatives CA16 and CA19] were injected by i.p every alternate day. Body weight and tumor growth were monitored every 2 days. GFP-expressing SW1 tumors were monitored *in vivo* on shaved mice with a light box illuminated by blue light fiber optics (Lightools Research), and imaging was carried out with a digital camera (Nikon D100). Tumors were measured for up to 3 weeks. For metastases studies, LU1205 cells (1×10^6) were injected i.v. into the lateral tail vein of nude mice. At the end of the experiment, the lungs and tumors were excised and weighted. To detect metastatic lesions, lungs were fixed in formalin, embedded in paraffin, and subjected to H&E staining.

Immunohistochemistry

Tumor sections (5 μm in thickness) were prepared and deparaffinized using xylene. Tumor sections were incubated in DAKO antigen retrieval solution for 20 min in a boiling bath followed by treatment with 3% hydrogen peroxide for 20 min. Antibodies against phosphorylated JNK (1:400) was allowed to react with tumor sections at 4°C overnight. Biotinylated anti-rabbit IgG was allowed to react for 30 min at room temperature and diaminobenzidine was used for the color reaction. Hematoxylin was used for counter-staining. The control sections were treated with normal rabbit serum.

Results

screening for compounds that mimic the ATF2 peptide effect on melanoma cells

We screened a chemical library of 3,280 pharmacologically active small molecules (33,34) to identify compounds that elicit the same major effects as the ATF2 peptide. The criteria for selection included the following: (*a*) the ability to elicit apoptosis of melanoma cells, (*b*) inhibition of ATF2 transcriptional activity, (*c*) increase in c-Jun transcriptional activity, and

(*d*) dependency on JNK activity. Compounds that met all four criteria were further assessed against a panel of melanoma cultures and in syngeneic and xenograft mouse models.

The screening was stepwise; thus, only compounds that met the first criterion were taken forward for further analyses to determine their effects on ATF2 and c-Jun transcriptional activities. Using this approach, 26 of the 3,280 compounds (0.8%) elicited efficient apoptosis of melanoma cells, which was monitored using the ATPLite assay. Of the 26 compounds, only 3 (0.1%) affected transcriptional activities of ATF2 and c-Jun. Because one of the three compounds was an organomercurial derivative (thimerasol), it was omitted from further analysis. Instead, more extensive studies were focused on CSL and acetyl isogambogic acid (AIGA), the two compounds that met the initial criteria.

Characterization of CSL and AIGA effects on mouse melanoma cells

The structures of AIGA and CSL are depicted inFig. 1A and B. AIGA was tested for cytotoxicity at concentrations ranging between 0.1 and 2 μmol/L, whereas CSL was used at a concentration of 0.01 to 0.3 μmol/L. Treatment of SW1 melanoma cells with 1 μmol/L AIGA reduced the viability of melanoma cells to 10% (Fig. 1C). Treatment of the SW1 cells with 0.05 μmol/L CSL reduced the viability of melanoma cells to 50%, and 0.1 μmol/L reduced it to 10% (Fig. 1C). These data suggest that both compounds elicit efficient cytotoxicity at a low micromolar concentration. Normal melanocytes and fibroblasts were used as a control. At the concentrations that efficiently induced cell death in melanoma cells, CSL caused minimal toxicity (10% at 0.1 μmol/L), whereas AIGA was more toxic (40% toxicity at the dose of 0.1 μmol/L) on normal mouse melanocytes (Fig. 1D). Neither CSL nor AIGA elicited toxic effect on human diploid fibroblasts (IMR90) or on the normal human breast cultures MCF10 (data not shown). These data suggest that CSL exhibits potent toxicity toward melanoma cultures but not toward nontransformed cells.

We next assessed the effects of the two compounds on c-Jun transcriptional activity in the mouse melanoma SW1 cells. Compared with the ATF2 peptide, which elicits an increase in TRE-luciferase, reflective of AP1/c-Jun transcriptional activity, AIGA and CSL elicited stronger activation of c-Jun transcription (Fig. 2A; Supplementary Fig. S1). AIGA induced c-Jun transcriptional activity at doses starting from 0.1 μmol/L (Supplementary Fig. S1). Compared with AIGA, CSL was more potent in the activation of AP1/c-Jun transcription, and as such, activation was seen in response to treatment at doses as low as 0.05 μmol/L (Fig. 2A). These compounds were next assessed for their effect on ATF2 transcriptional activity. About 0.5 μmol/L AIGA or 0.05 μmol/L CSL was required to cause ~ 50% inhibition of ATF2 transcriptional activity, monitored using a Jun2-luciferase construct (Fig. 2B; Supplementary Fig. S2). These data reveal that, similar to the changes seen after treatment with the ATF2 peptide, both compounds effectively alter the transcriptional activities of ATF2 and c-Jun, although CSL seems to be more potent compared with AIGA.

To assess whether CSL may affect the transcriptional activities of genes other than ATF2 and c-Jun, we monitored possible changes in transcriptional activities of nuclear factor-κB (NF-κB). Addition of either AIGA or CSL causes dose-dependent inhibition of NF-κB transcriptional activity, measured by the corresponding luciferase reporter construct (Supplementary Figs. S3 and S4). These findings are consistent with earlier reports about the effect of CSL on the transcriptional activities of NF-κB in HeLa cells (36).

To assess the possible effect of these compounds on other signaling pathways, we have monitored changes in the phosphorylation of AKT and ERK. CSL treatment of melanoma cells caused activation of AKT and ERK phosphorylation, suggesting a more global effect on stress-induced signaling (Supplementary Fig. S5).

Our earlier studies have revealed that JNK activity is central to the ability of the ATF2 peptide to elicit its effect on melanoma cells in culture and *in vivo* (inhibition of tumorigenicity). We therefore assessed whether the two compounds identified in the present study require JNK activity for their effects on melanoma cells. To this end, we first tested the ability of AIGA or CSL to affect the viability of melanoma cells in the presence of a JNK inhibitor. Inhibition of JNK activity by the pharmacologic inhibitor SP600125 attenuated the ability of AIGA or CSL to elicit the cell death of melanoma cells (Fig. 2C; Supplementary Fig. S6). Of note, inhibition of JNK activity was more pronounced at lower concentrations of CSL compared with AIGA. These findings suggest that AIGA and CSL require JNK activity to reduce the survival of melanoma cells.

To assess whether these compounds affect JNK activity, we monitored changes in JNK phosphorylation on residues 183/185, which are required for its kinase activity. Both AIGA and CSL induced phosphorylation of JNK on these residues, which was reduced on addition of the JNK inhibitor (Fig. 2D; Supplementary Fig. S7). The activation of JNK by both compounds was confirmed on analysis of its substrate c-Jun. Both compounds efficiently induced c-Jun phosphorylation, with CSL being more potent (Fig. 2D). These data indicate that CSL and AIGA induce JNK activity, which in turn results in the activation of its substrate c-Jun while attenuating the degree of ATF2 transcriptional activity.

The finding that CSL and AIGA reduced cell viability in melanoma was made using the ATPLite assay, which monitors the degree of mitochondrial ATP release, a marker for mitochondrial activity. To directly assess possible changes in the apoptosis of melanoma cells following their exposure to CSL or AIGA, we have done fluorescence-activated cell sorting analysis of the melanoma cells 48 h after treatment. Addition of AIGA or CSL to SW1 melanoma cells induced programmed cell death, with CSL exhibiting a more efficient effect. Treatment with 1 Amol/L AIGA caused 15% apoptosis in these melanoma cultures (Fig. 3A). Treatment with CSL caused 13% apoptosis at a dose of 0.5 μmol/L and 35% apoptosis at a dose of 1 μmol/L (Fig. 3A). Consistent with these finding is the activation of caspase-8, which was observed on addition of these compounds (Fig. 3B).

Effects of CSL and AIGA on human melanoma cells

Given the effects of CSL and AIGA on mouse melanoma cells, we next assessed their effects on the human melanoma cell lines WM115 and MEWO. AIGA reduced the viability of the human melanoma cultures when added at a concentration of 0.5 to 2 μmol/L, whereas CSL reduced their viability at a concentration of 1 μmol/L (Fig. 3C and D). These data reveal that, similar to their effect on the mouse melanoma cells, AIGA and CSL efficiently reduced viability of human melanoma cells.

Generation and characterization of CSL derivatives that affect melanoma cells

Given the greater potency of CSL, compared with AIGA, on transcription and cell death, we have devoted efforts to further optimize the ability of CSL to elicit melanoma cell death. To this end, medicinal chemistry was initiated with the dual goals of (*a*) understanding the key structural features in CSL that affect its apoptotic activity and (*b*) identifying analogues of CSL that possess an improved pharmacologic profile compared with the parent compound. To this end, we first tested two commercially available analogues of CSL, the CSL methyl ester (pristimerin) and dihydrocelastrol, a reduced variant of CSL that lacks the quinone methide moiety in the parent compound. Pristimerin was equipotent or even slightly more potent than CSL (see Table 1) against SW1 cells. This finding suggests that the acidic proton present in CSL is not required for its ability to induce apoptosis in these cells. Dihydrocelastrol, however, was inactive in the assay, suggesting that the quinone methide moiety in CSL is crucial for apoptotic activity (see Discussion). With this information in hand, we focused on modification

of the carboxylic acid moiety in CSL. We first synthesized a series of amide derivatives (CA01–CA08, CA13, and CA14) and these were tested in the cellular assays as shown in Table 1. This set of amides was designed to interrogate both the steric and electronic requirements of the carboxylate substitute needed for optimal cellular activity. The derivatives revealed some intriguing preliminary structure-activity relationship data (Table 1). The 4-methoxybenzyl amide (CA01) and the pyridin-3-ylmethanamine amide (CA03) were active in SW1 cells, whereas the unsubstituted benzyl amide (CA02) was inactive. Among the aliphatic amides, the isopropyl amide (CA04), the dimethyl amide (CA05), the pyrrolidine amide (CA06), and the methoxyethyl-amine (CA07) were all active in SW1 cells. However, the morpholine amide (CA08) and the *N*-methylpiperazine amide (CA14) were both inactive. Surprisingly, considering the dimethyl amide (CA05) result, the monomethyl amide (CA13) was also inactive (Table 1). This suggested that the presence of an amide N-H reduces cellular activity in this series.

These observations prompted us to synthesize and test some ester derivatives based on the rationale that, unlike primary amides, esters lack a heteroatom proton. Thus, the methyl 2-hydroxyacetate ester (CA15), the benzyl ester (CA16), the ethyl ester (CA18), and the isopropyl ester (CA19) were prepared and the cellular assay data are shown in Table 1. Among these four derivatives, two (CA16 and CA19) potently exhibited the ability to induce melanoma cell death. CA18 was not that efficient in the SW1 melanoma cells compared with CA19. Remarkably, the benzyl ester (CA16) was quite potent compared with the corresponding amide derivative (CA02), which was inactive. Taken together, these results suggest that the ester derivatives are more potent than the corresponding amide derivatives. Based on these data, the CA16 and CA19 derivatives were selected as representatives for further assessment in the syngeneic and xenograft mouse models.

Evaluation of CSL and its derivatives in melanoma tumorigenicity

To assess the ability of CSL and its derivatives to affect the tumorigenicity and metastasis of melanoma, we used the mouse SW1 cell lines in syngeneic models. Injection of SW1 melanoma cells s.c. into C3H mice was followed by i.p. injections of CSL on alternate days. Importantly, administration of CSL, CA16, or CA19 to mice at doses up to 1 mg/kg did not result in toxicity or any noticeable discomfort, indicating that these compounds are well tolerated and not toxic at these high doses. Significantly, CSL attenuated the growth of both mouse and human melanoma cells *in vivo* using immunocompetent and immunodeficient mouse models (Figs. 4 and 5). Comparison of CSL, CA16, and CA19 for their effects on the viability of SW1 cells in culture revealed that both derivatives were as potent as the parent CSL compound (Fig. 4A). Administration of these compounds, compared with vehicle control, revealed that both CSL and the derivatives attenuated growth of SW1 tumors in mice (Fig. 4B). Interestingly, CSL and CA19 were equally potent and reduced tumor growth 5-fold, whereas CA16 was less effective in inhibiting tumor size (~ 50% decrease; Fig. 4B). Representative figures of GFP-labeled tumors in animals treated with control or CSL show the effect of these compounds after 3 weeks of treatment (Fig. 4C). The effect of CSL on tumors that were excised from these animals is also shown (Fig. 4C). Consistent with our finding in cultured cells, CSL treatment also induced JNK activity in the tumors; such activity was not observed in the vehicle-treated tumors (Fig. 4D), thereby supporting the changes seen in the SW1 cultures. These data suggest that CSL and its derivatives efficiently reduce melanoma tumor growth in a syngeneic mouse model.

We next determined the possible effect of CSL and the selected derivatives on the metastatic capacity of melanoma cells. To this end, human melanoma LU1205 cells were subjected to tail vein injection followed by administration of the compounds every second day. This approach allows monitoring of changes in the number of lesions formed on the lungs, a primary

organ for tumor cell growth under this experimental approach. Analysis done 60 days following injection determined changes in the number and size of metastatic lesions in each of the experimental groups. Significantly, CSL and CA19 were efficient in inhibiting growth of large-, medium-, and small-sized lesions in the lungs (Fig. 5A). CA16 had no effect on the development of the large lesions, although some activity was observed for 1 to 2 mm and for mediastinal lesions (Fig. 5A). These data suggest that the compounds are capable of inhibiting metastasis of human melanoma cells in a nude mouse model and that at least one of the two derivatives tested here, CA19, exhibits potent activity that is comparable with CSL.

To further assess the effect of these compounds on the development of metastatic lesions, we turned to the SW1 mouse melanoma model using the syngeneic C3H strain. S.c. injection of SW1 cells results in tumor formation at the site of injection followed by metastasis to different sites within 6 to 8 weeks (31). Similar to what was observed with the human melanoma cells in the nude mice model, CSL and CA19 potently exhibit the ability to inhibit large as well as small metastatic lesions, with the exception of the 1-to 2-mm range (Fig. 5B), whereas CA16 was somewhat active it elicited an opposite effect on the development of small-sized lesions (Fig. 5B). The fluctuations seen with CA16 imply that its activity may be limited due to stability or permeability. These data provide important support for the ability to attenuate tumorigenicity and metastatic lesion formation in melanoma xenograft and syngenic models using CSL and its isopropyl ester derivative CA19.

Discussion

The present study extends earlier reports that documented the ability of the ATF2 peptide to cause apoptosis in mouse and human melanoma cells in culture and in animal models (29–32). To identify compounds that mimic the activity of the ATF2 peptide, we screened a small-molecule chemical library consisting of 3,280 compounds. Two compounds, CSL and AIGA, at low micromolar concentrations, were able to (*a*) induce melanoma cell death, (*b*) inhibit the transcriptional activity of ATF2, and (*c*) induce the activity of JNK and transcriptional activity of c-Jun and required active JNK for their ability to affect melanoma viability.

Gambogic acid was originally isolated from the resin of the *Garcinia hanburyi* tree, whose cytotoxic properties are recognized (37). In recent studies, AIGA was shown to possess the capacity to potently induce apoptosis in a breast cancer cell line T47D (38), in a human hepatoma cell line SMMC-7721 (39), and in a gastric carcinoma cell line BGC-823, in part through G_2-M phase arrest (40). Consistent with these findings, we show herein that AIGA elicits potent inhibition of melanoma cell growth in culture. We further show that AIGA elicits these effects in part through activation of JNK and c-Jun and inhibition of ATF2.

CSL, a quinone methide triterpenoid isolated from the Chinese “thunder of god vine” plant, was reported to exhibit immunosuppressive activities (41). CSL was also shown to induce the heat shock response and to elicit cytoprotection (42). Consistent with these findings, gene expression signature-based chemical genomic prediction identified CSL as a modulator of the HSP90 pathway (43). At micromolar concentrations, CSL was shown capable of inhibiting proteasome activity and the growth of prostate cancer cells in nude mice (44). At the concentrations used in the present studies (0.3–1 μmol/L), CSL did not affect the stability of short-lived proteins, including Mdm2 and p53 (data not shown). CSL was also shown to inhibit NF-κB activation through the inhibition of IκB kinase (36) and TAK1 activities (45). Previous studies showed that NF-κB inhibits JNK activities and that inhibition of NF-κB results in elevated JNK activities (46–49). Thus, it is likely that the ability of CSL to attenuate NF-κB activity would result in increased JNK activity, which is consistent with our findings. It is the increase in JNK activity, and consequently of its substrate c-Jun, in concert with inhibition of

ATF2 activities that brings about the potent cytotoxic effects of both CSL and AIGA on melanoma cells, similar to what was previously shown for the ATF2 peptides (29–32,50).

The greater apoptotic effects seen with CSL compared with AIGA in cultured cells prompted us to focus on CSL. Examination of the structure of CSL led us to postulate that the quinone methide functional group was responsible for its cytotoxic activity. Along these lines, we reasoned that the highly electrophilic nature of the quinone methide unit could potentially lead to irreversible or pseudo-irreversible binding to proteins, possibly through interaction with cysteinyl residues. Supporting this hypothesis is the fact that dihydrocelastrol, which lacks the quinone methide moiety, is inactive in the cellular assays (Table 1). On the other hand, the methyl ester derivative of CSL (pristimerin) is equally efficacious as CSL with respect to its ability to induce apoptosis, suggesting that the presence of the acidic carboxylate functional group in CSL is not required for apoptotic activity but that the quinone methide moiety is responsible for the observed cellular activity in our experiments. Data recently reported by Westerheide et al. (42) support this hypothesis and further suggest that the carboxylic acid moiety in CSL is responsible for the chemical chaperone activity observed in their experiments. Thus, in the study conducted by Westerheide et al. (42), three ester derivatives of CSL were inactive as regulators of the heat shock response, whereas dihydrocelastrol was active as a heat shock promoter. These results suggest that the quinone methide moiety is not responsible for the observed chemical chaperone activity. We therefore synthesized a series of CSL derivatives in which the carboxylic acid unit in CSL was converted to an amide or ester derivative with the quinone methide functional group retained intact in the molecules (see Results). Consistent with a role for the quinone methide unit in the cytotoxicity of CSL, some of the CSL derivatives exhibited improved efficacy (Table 1). These results led to the identification of the benzyl ester (CA16) and isopropyl ester (CA19) derivatives as potent inducers of apoptosis, which were profiled in detail in *in vivo* models of melanoma. The precise role for the carboxylic acid moiety in this modality of CSL remains to be further elucidated, however.

Consistent with its ability to induce apoptosis of melanoma cells in culture is the ability of CSL and its isopropyl ester derivative CA19 to attenuate the growth of melanoma in mouse models. Our analysis, which was done in syngeneic mouse (SW1 cells in C3H mice) and human xenograft (LU1205 in nude mice) models, shows the ability of these compounds to attenuate growth of metastatic lesions, which are the major clinical burden in treatment of this tumor type. The lower activity of CA16 compared with CA19 and CSL on tumor growth and metastasis development may be attributed to stability or permeability of this compound *in vivo*. Along these lines, in all cases, it was necessary to inject the compounds at high frequency; it is expected that improved formulation will allow prolonged half-life and more efficient delivery of these compounds. The low concentrations of the compounds used in our present studies would be expected to minimize effect on other organs, consistent with our initial maximum tolerated dose studies.

In conclusion, the effects of AIGA and CSL on melanoma cells in culture and in mouse models point to possible new treatment modalities for melanoma. In light of the notion that MAPK signaling is up-regulated in human melanoma, in many cases as a result of mutations in *B-RAF* or *N-RAS*, our findings suggest that these compounds could be also considered as a means of complementing the activities of pharmacologic inhibitors developed against MAPK/ERK kinase.

Supplementary Material

Refer to Web version on PubMed Central for supplementary material.

Acknowledgments

We thank M. Herlyn for providing us with the melanoma cell lines, members of the Ronai Lab for discussions, Dr. Marcia Dawson for critical comments, Buddy Charbono for help in injection in the mice, and Robbin Newlin for help in preparation of histologic samples.

Grant support: National Cancer Institute grant CA099961 (Z.A. Ronai).

References

1. Chin L, Garraway LA, Fisher DE. Malignant melanoma: genetics and therapeutics in the genomic era. Genes Dev 2006;20:2149–2182. [PubMed: 16912270]
2. Reed JA, Medrano EE. Recent advances in melanoma research. Front Biosci 2006;11:3003–3013. [PubMed: 16720371]
3. Meier F, Schittek B, Busch S, et al. The RAS/RAF/MEK/ERK and PI3K/AKT signaling pathways present molecular targets for the effective treatment of advanced melanoma. Front Biosci 2005;10:2986–3001. [PubMed: 15970553]
4. Halaban R. Rb/E2F: a two-edged sword in the melanocytic system. Cancer Metastasis Rev 2005;24:339–356. [PubMed: 15986142]
5. Curtin JA, Fridlyand J, Kageshita T, et al. Distinct sets of genetic alterations in melanoma. N Engl J Med 2005;353:2135–2147. [PubMed: 16291983]
6. Goel VK, Lazar AJ, Warneke CL, Redston MS, Haluska FG. Examination of mutations in BRAF, NRAS, and PTEN in primary cutaneous melanoma. J Invest Dermatol 2006;126:154–160. [PubMed: 16417231]
7. Gorden A, Osman I, Gai W, et al. Analysis of BRAF and N-RAS mutations in metastatic melanoma tissues. Cancer Res 2003;63:3955–3957. [PubMed: 12873990]
8. Levy C, Khaled M, Fisher DE. MITF: master regulator of melanocyte development and melanoma oncogene. Trends Mol Med 2006;12:406–414. [PubMed: 16899407]
9. Goding CR. Mitf from neural crest to melanoma: signal transduction and transcription in the melanocyte lineage. Genes Dev 2000;14:1712–1728. [PubMed: 10898786]
10. Ellerhorst JA, Ekmekcioglu S, Johnson MK, Cooke CP, Johnson MM, Grimm EA. Regulation of iNOS by the p44/42mitogen-activated protein kinase pathway in human melanoma. Oncogene 2006;25:3956–3962. [PubMed: 16474847]
11. Bhatt KV, Spofford LS, Aram G, McMullen M, Pumiglia K, Aplin AE. Adhesion control of cyclin D1 and p27Kip1 levels is deregulated in melanoma cells through BRAF-MEK-ERK signaling. Oncogene 2005;24:3459–3471. [PubMed: 15735667]
12. Robertson GP. Functional and therapeutic significance of Akt deregulation in malignant melanoma. Cancer Metastasis Rev 2005;24:273–285. [PubMed: 15986137]
13. Bedogni B, Welford SM, Cassarino DS, Nickoloff BJ, Giaccia AJ, Powell MB. The hypoxic microenvironment of the skin contributes to Akt-mediated melanocyte transformation. Cancer Cell 2005;8:443–454. [PubMed: 16338658]
14. Lopez-Bergami P, Habelhah H, Bhoumik A, Zhang W, Wang LH, Ronai Z. RACK1 mediates activation of JNK by protein kinase C [corrected]. Mol Cell 2005;19:309–320. [PubMed: 16061178]
15. Gillespie S, Zhang XD, Hersey P. Variable expression of protein kinase Cε in human melanoma cells regulates sensitivity to TRAIL-induced apoptosis. Mol Cancer Ther 2005;4:668–676. [PubMed: 15827341]
16. Lahn MM, Sundell KL. The role of protein kinase C-α (PKC-α) in melanoma. Melanoma Res 2004;14:85–89. [PubMed: 15057036]
17. Chin L, Pomerantz J, Polsky D, Jacobson M, Cohen C, Cordon-Cardo C, Horner JW 2nd, DePinho RA. Cooperative effects of INK4a and ras in melanoma susceptibility *in vivo*. Genes Dev 1997;11:2822–2834. [PubMed: 9353252]
18. Hussussian CJ, Struewing JP, Goldstein AM, et al. Germline p16 mutations in familial melanoma. Nat Genet 1994;8:15–21. [PubMed: 7987387]

19. Carreira S, Goodall J, Aksan I, et al. Mitf cooperates with Rb1 and activates p21Cip1 expression to regulate cell cycle progression. Nature 2005;433:764–769. [PubMed: 15716956]
20. Melnikova VO, Mourad-Zeidan AA, Lev DC, Bar-Eli M. Platelet-activating factor mediates MMP-2 expression and activation via phosphorylation of cAMP-response element-binding protein and contributes to melanoma metastasis. J Biol Chem 2006;281:2911–2922. [PubMed: 16306050]
21. Hofmann UB, Houben R, Brocker EB, Becker JC. Role of matrix metalloproteinases in melanoma cell invasion. Biochimie 2005;87:307–314. [PubMed: 15781317]
22. McGary EC, Lev DC, Bar-Eli M. Cellular adhesion pathways and metastatic potential of human melanoma. Cancer Biol Ther 2002;1:459–465. [PubMed: 12496470]
23. Grbovic OM, Basso AD, Sawai A, et al. V600EB-Raf requires the Hsp90 chaperone for stability and is degraded in response to Hsp90 inhibitors. Proc Natl Acad Sci U S A 2006;103:57–62. [PubMed: 16371460]
24. Jean D, Harbison M, McConkey DJ, Ronai Z, Bar-Eli M. CREB and its associated proteins act as survival factors for human melanoma cells. J Biol Chem 1998;273:24884–24890. [PubMed: 9733794]
25. Ronai Z, Yang YM, Fuchs SY, Adler V, Sardana M, Herlyn M. ATF2 confers radiation resistance to human melanoma cells. Oncogene 1998;16:523–531. [PubMed: 9484842]
26. Berger AJ, Davis DW, Tellez C, et al. Automated quantitative analysis of activator protein-2α subcellular expression in melanoma tissue microarrays correlates with survival prediction. Cancer Res 2005;65:11185–11192. [PubMed: 16322269]
27. Lopez-Bergami P, Huang C, Goydos S, et al. Rewired ERK-JNK signaling pathways in melanoma. Cancer Cell 2007;11:447–460. [PubMed: 17482134]
28. Berger AJ, Kluger HM, Li N, et al. Subcellular localization of activating transcription factor 2 inmelanoma specimens predicts patient survival. Cancer Res 2003;63:8103–8107. [PubMed: 14678960]
29. Bhoumik A, Ivanov V, Ronai Z. Activating transcription factor 2-derived peptides alter resistance of human tumor cell lines to ultraviolet irradiation and chemical treatment. Clin Cancer Res 2001;7:331–342. [PubMed: 11234888]
30. Bhoumik A, Gangi L, Ronai Z. Inhibition of melanoma growth and metastasis by ATF2-derived peptides. Cancer Res 2004;64:8222–8230. [PubMed: 15548688]
31. Bhoumik A, Huang TG, Ivanov V, et al. An ATF2-derived peptide sensitizes melanomas to apoptosis and inhibits their growth and metastasis. J Clin Invest 2002;110:643–650. [PubMed: 12208865]
32. Bhoumik A, Jones N, Ronai Z. Transcriptional switch by activating transcription factor 2-derived peptide sensitizes melanoma cells to apoptosis and inhibits their tumorigenicity. Proc Natl Acad Sci U S A 2004;101:4222–4227. [PubMed: 15010535]
33. Hamman BD, Pollok BA, Bennett T, Allen J, Heim R. Binding of a pleckstrin homology domain protein to phosphoinositide in membranes: a miniaturized FRET-based assay for drug screening. J Biomol Screen 2002;7:45–55. [PubMed: 11897055]
34. Kocisko DA, Baron GS, Rubenstein R, Chen J, Kuizon S, Caughey B. New inhibitors of scrapie-associated prion protein formation in a library of 2,000 drugs and natural products. J Virol 2003;77:10288–10294. [PubMed: 12970413]
35. Kangas L, Grönroos M, Nieminen AL. Bioluminescence of cellular ATP: a new method for evaluating agents *in vitro*. Med Biol (Helsinki) 1984;62:338–343.
36. Lee JH, Koo TH, Yoon H, et al. Inhibition of NF-κB activation through targeting IκB kinase by celastrol, a quinone methide triterpenoid. Biochem Pharmacol 2006;72:1311–1321. [PubMed: 16984800]
37. Asano J, Chiba K, Tada M, Yoshii T. Cytotoxic xanthones from *Garcinia hanburyi*. Phytochemistry 1996;41:815–820. [PubMed: 8835458]
38. Zhang HZ, Kasibhatla S, Wang Y, et al. Discovery, characterization and SAR of gambogic acid as a potent apoptosis inducer by a HTS assay. Bioorg Med Chem 2004;12:309–317. [PubMed: 14723951]
39. Guo QL, You QD, Wu ZQ, Yuan ST, Zhao L. General gambogic acids inhibited growth of human hepatoma SMMC-7721cells *in vitro* and in nude mice. Acta Pharmacol Sin 2004;25:769–774. [PubMed: 15169630]

40. Jun Y, Guo QL, You QD, et al. Gambogic acid induced G_2/M phase cell cycle arrest via disturbing CDK7 mediated phosphorylation of CDC2/P34 in humangastric carcinomaBGC-823 cells. Carcinogenesis 2007;28:632–638. [PubMed: 17012222]
41. Zhou BN. Some progress on the chemistry of natural bioactive terpenoids from Chinese medicinal plants. Mem Inst Oswaldo Cruz 1991;86:219–226. [PubMed: 1842005]
42. Westerheide SD, Bosman JD, Mbadugha BN, et al. Celastrols as inducers of the heat shock response and cytoprotection. J Biol Chem 2004;279:56053–56060. [PubMed: 15509580]
43. Hieronymus H, Lamb J, Ross KN, et al. Gene expression signature-based chemical genomic prediction identifies a novel class of HSP90 pathway modulators. Cancer Cell 2006;10:321–330. [PubMed: 17010675]
44. Yang H, Chen D, Cui QC, Yuan X, Dou QP. Celastrol, a triterpene extracted from the Chinese “Thunder of God Vine,” is a potent proteasome inhibitor and suppresses human prostate cancer growth in nude mice. Cancer Res 2006;66:4758–4765. [PubMed: 16651429]
45. Sethi G, Ahn KS, Pandey MK, Aggarwal BB. Celastrol, a novel triterpene, potentiates TNF-induced apoptosis and suppresses invasion of tumor cells by inhibiting NF-κB-regulated gene products and TAK1-mediated NF-κB activation. Blood 2007;109:2727–2735. [PubMed: 17110449]
46. Javelaud D, Besancon F. NF-κB activation results in rapid inactivation of JNK in TNFα-treated Ewing sarcoma cells: a mechanism for the anti-apoptotic effect of NF-κB. Oncogene 2001;20:4365–4372. [PubMed: 11466617]
47. Tang G, Minemoto Y, Dibling B, et al. Inhibition of JNK activation through NF-κB target genes. Nature 2001;414:313–317. [PubMed: 11713531]
48. Eliseev RA, Zuscik MJ, Schwarz EM, O’Keefe RJ, Drissi H, Rosier RN. Increased radiation-induced apoptosis of Saos2 cells via inhibition of NFκB: a role for c-Jun N-terminal kinase. J Cell Biochem 2005;96:1262–1273. [PubMed: 16167336]
49. Wullaert A, Heyninck K, Beyaert R. Mechanisms of crosstalk between TNF-induced NF-κB and JNK activation in hepatocytes. Biochem Pharmacol 2006;72:1090–1101. [PubMed: 16934229]
50. Ivanov VN, Fodstad O, Ronai Z. Expression of ring finger-deleted TRAF2 sensitizes metastatic melanoma cells to apoptosis via up-regulation of p38,TNF α and suppression of NF-κB activities. Oncogene 2001;20:2243–2253. [PubMed: 11402319]

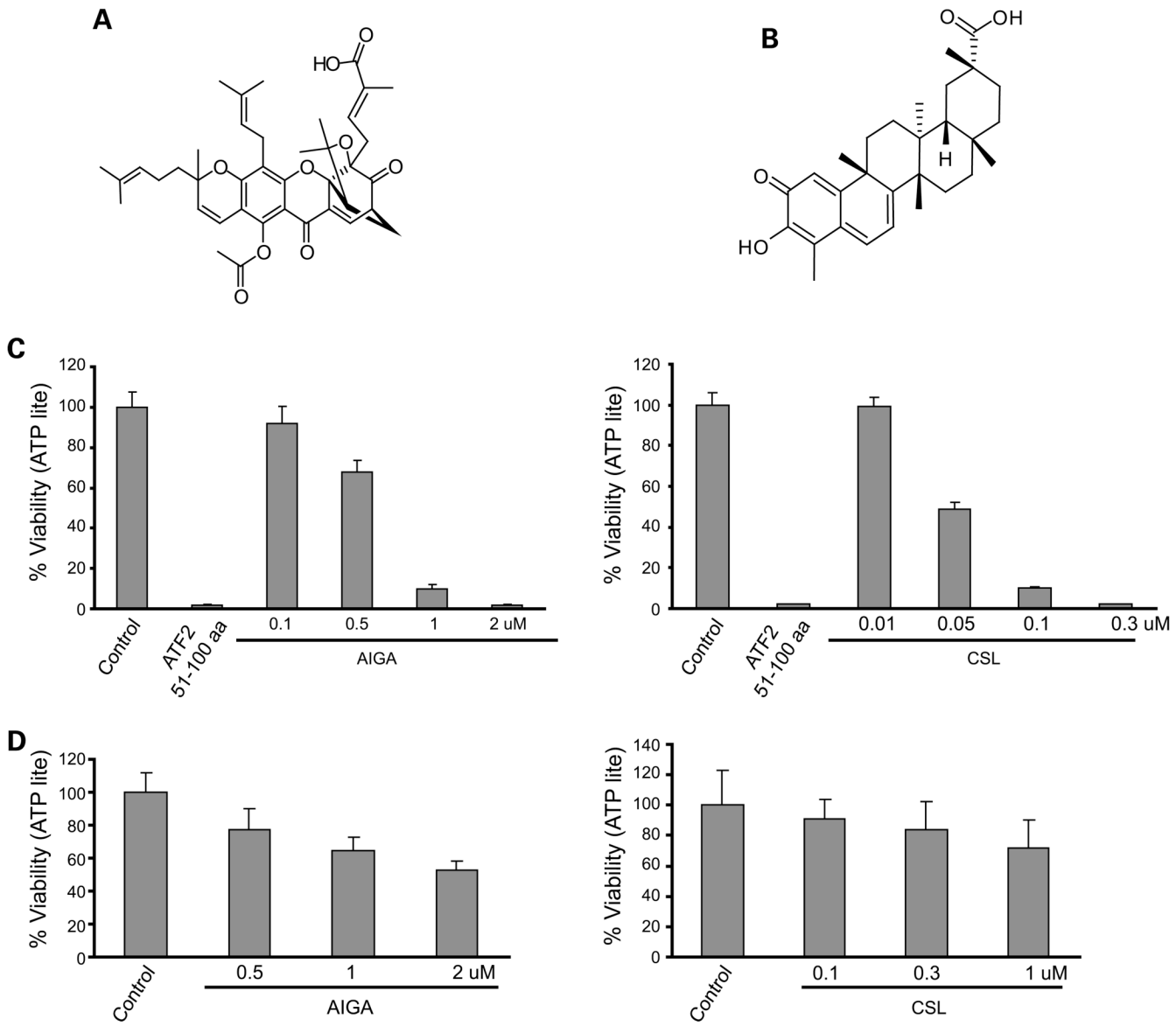

Fig. 1.

AIGA and CSL reduces cell viability of SW1mouse melanoma cells. *A*, chemical structure of AIGA. *B*, chemical structure of CSL. *C*, SW1 cells were seeded on 96-well plates, and 24 h later, cells were treated with the indicated doses of AIGA or CSL for 20 h. $ATF2^{51–100}$ peptide (cloned in mammalian expression vector in frame with penetratin was transfected with the aid of Lipofectamine as described in ref. 31) was used as a positive control. ATP levels were used as an indicator of cell viability using the ATPLite kit. The number of surviving cells on AIGA or CSL treatment was normalized to the number of surviving cells under the control treatment, and the normalized number was designated as the "CellViability (%)",which is represented by the *Y* axis. Results shown represent three experiments ($P < 0.005$ for AIGA and $P < 0.0045$ for CSL). *D*, experiment was done as indicated in *C*, except that normal melanocytes were used for the analysis ($P < 0.01$ for AIGA and $P < 0.05$ for CSL).

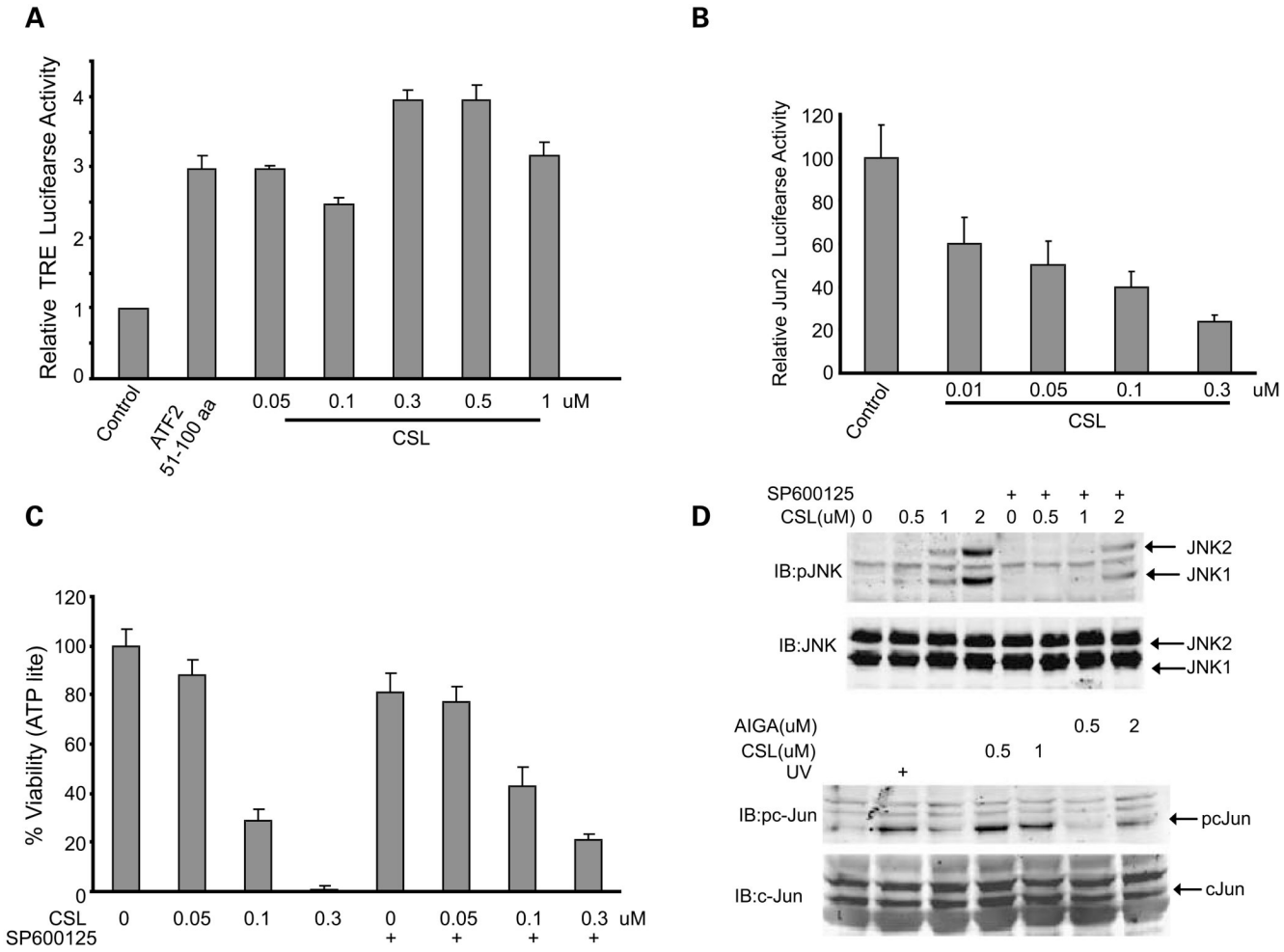

Fig. 2.

AIGA and CSL increase JNK and c-Jun and reduce ATF2 activities. *A*, SW1 cells were transfected with the TRE-luciferase plasmid, and 24 h later, cells were treated with the indicated doses of CSL for 8 h before proteins were prepared and level of luciferase activity was measured. $ATF2^{51–100}$ peptide was used as a positive control. Data represent results from three experiments ($P < 0.005$). *B*, the effect of CSL on Jun2-luciferase activity was assessed, as detailed in *A*. Data represent results from three experiments ($P < 0.003$). *C*, SW1 cells were pretreated (for 30 min) with the JNK inhibitor SP600125 (10 μmol/L) followed by addition of CSL for 20 h. ATP levels were used to measure the cell viability using the ATPLite kit. Calculation for altered viability was done as detailed in legend to Fig.1C. Representative results from two experiments ($P < 0.02$). *D*, top, Western blot analysis for JNK phosphorylation (*pJNK*) on residues 183/185 was done on protein extracts that were prepared from cells treated with CSL, as indicated in *A*; bottom, total level of JNK. SW1 cells were pretreated with the JNK inhibitor SP600125 followed by addition of AIGA or CSL for 20 h, as indicated in *A* and *B*. Total protein extracts were used to determine the phosphorylation of c-Jun (*pc-Jun*).

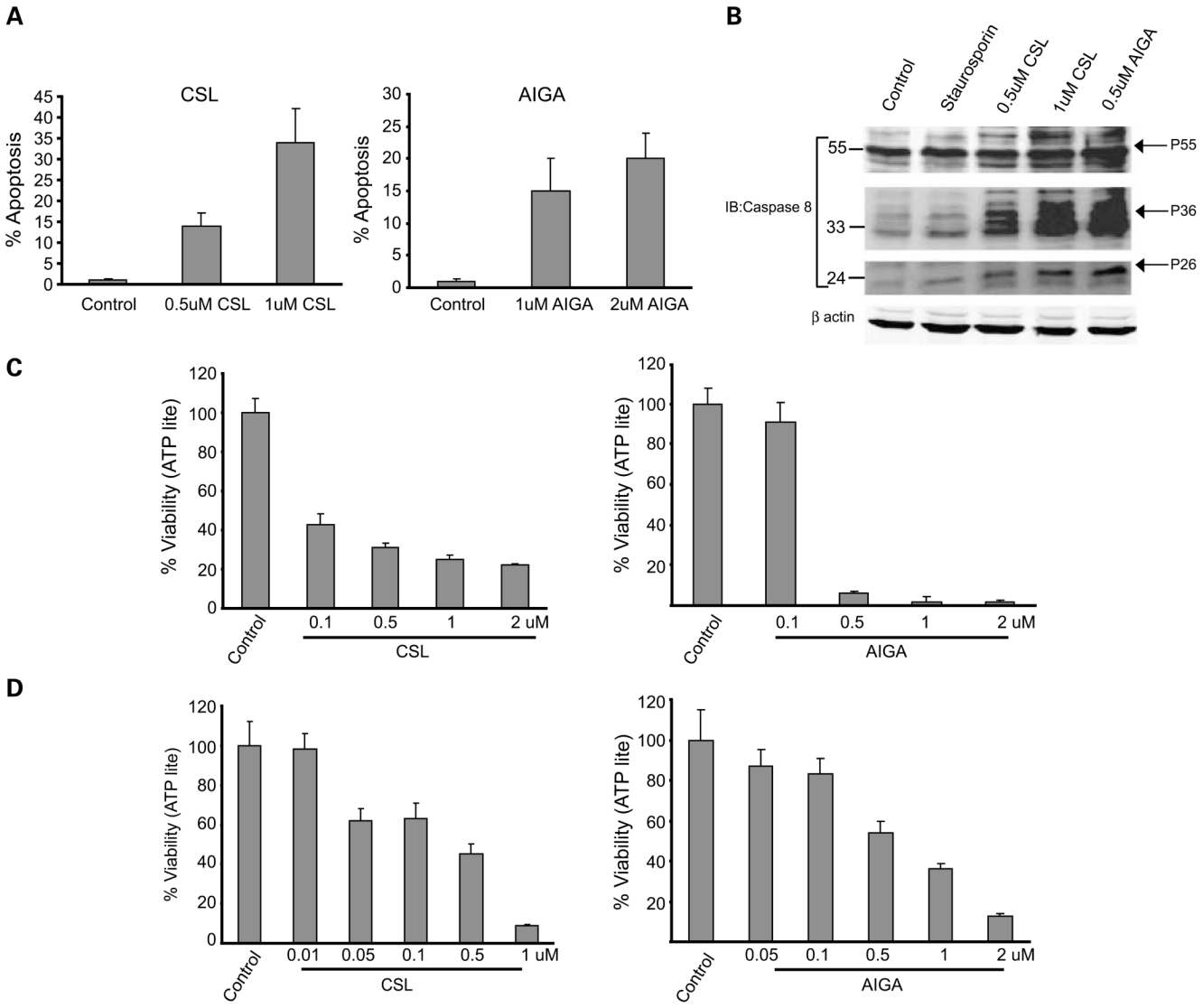

Fig. 3.

AIGA and CSL induce apoptosis in melanoma cells. *A*, SW1 cells were treated with CSL or AIGA at the indicated concentrations, and the degree of apoptosis, measured by fluorescence-activated cell sorting analysis, was determined 48 h later. Data represent three different experiments. *B*, SW1 cells were treated with AIGA or CSL at the indicated doses for 24 h. Staurosporine was used as a positive control. Immunoblot analysis using caspase-8 antibody monitored full-length and cleaved forms (active) of caspase-8. β-Actin was used as a loading control. The positions of the cleaved forms are indicated. *C* and *D*, human melanoma WM115 (*C*) or MEWO (*D*) cells were treated with the indicated doses of CSL or AIGA for 20 h. ATP levels were used to measure the cell viability using the ATPLite kit. Calculation was done as detailed in legend to Fig.1C. Representative results from three experiments.

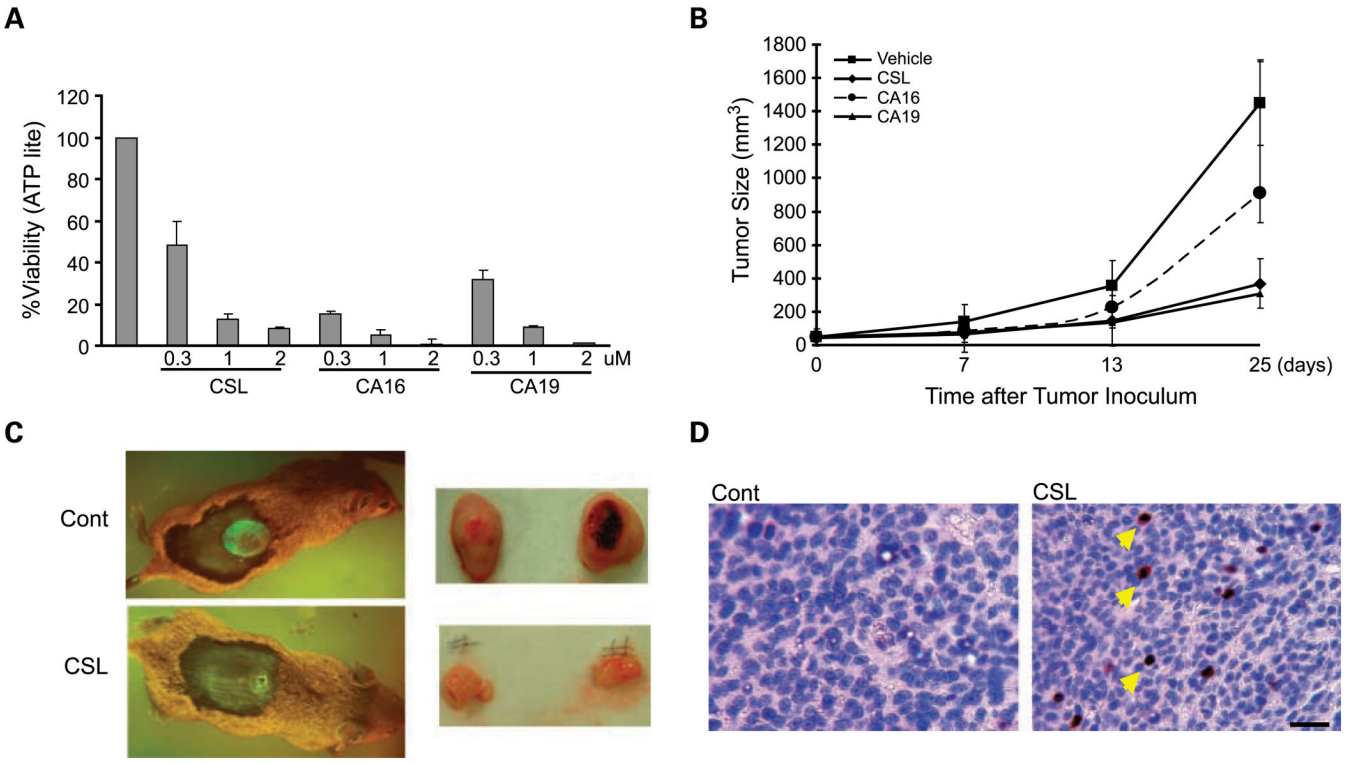

Fig. 4.

CSL and CSL derivatives, CA16 and CA19, reduce cell viability *in vitro* and attenuate tumor growth *in vivo*. *A*, SW1 cells were seeded on 96-well plates, and after 24 h, cells were treated with the indicated doses of CSL and the select derivatives CA16 and CA19 for 20 h. ATP levels were used to measure the cell viability using the ATPLite kit. Calculation of viability was done as detailed in Fig.1C. Representative results are from three independent experiments. *B*, SW1 cells that stably express GFP were injected s.c into C3H mice. When the tumor reached the size of 50 mm^3, the vehicle, CSL (1mg/kg), CA16 (0.5 mg/kg), or CA19 (0.5 mg/kg) was given i.p. every second day for a period of 24 d. Tumor was measured at the indicated times. Data represent two experiments. Bars, SD. $P < 0.005$, *t* test. $n = 7$. *C*, representative figures of mice with GFP tumors formed in C3H mice (*left panel*) or of the tumors excised from the xenograft model in nude mice (*right panel*). *D*, tumors detailed in Fig. 5B were excised and paraffin sections were prepared and stained with phosphorylated JNK antibody. Bar, 50 μm. Arrows point to examples of phosphorylated JNK – positive cells.

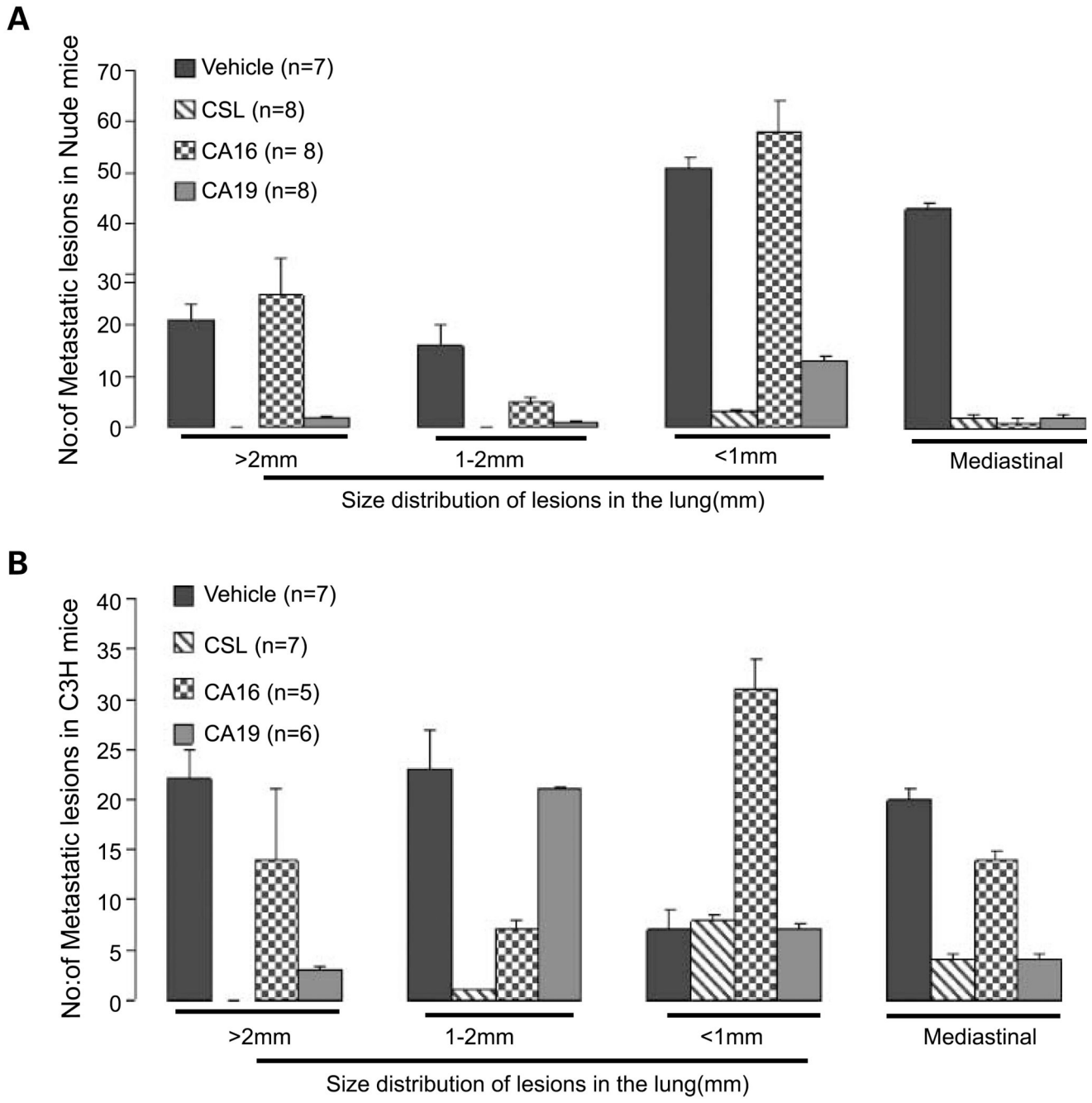

Fig. 5.

CSL and CSL derivatives, CA16 and CA19, attenuate tumor metastasis *in vivo*. *A*, CSL, CA16, or CA19 inhibits lung lesions of human LU1205 cells. Tail vein injection of human melanoma LU1205 cells was followed by analysis of lung lesions. The effect of these compounds on the number and size of lesions obtained after H&E staining on serial sections of lungs was calculated. Average number of lesions was calculated within serial sections of the lungs from every mouse in two independent experiments. $n = 10$. *B*, CSL, CA16, or CA19 inhibits lung metastasis of SW1 tumor. S.c. injection of SW1 cells resulted in tumors (Fig. 4B) that within 6 to 8 wk metastasize to the lungs (29). Average number of metastatic lesions in the lungs and the mediastinal lesions was calculated based on analysis of several sections representing

different longitudinal sections within the lungs. The change in metastatic lesions was divided based on the size of the lesions, as indicated in *A*. Data represent average of two experiments. $n = 7$

Table 1

Activity of CSL derivatives

Code	Structure	Activ EC_{50} (I in SW
CSL	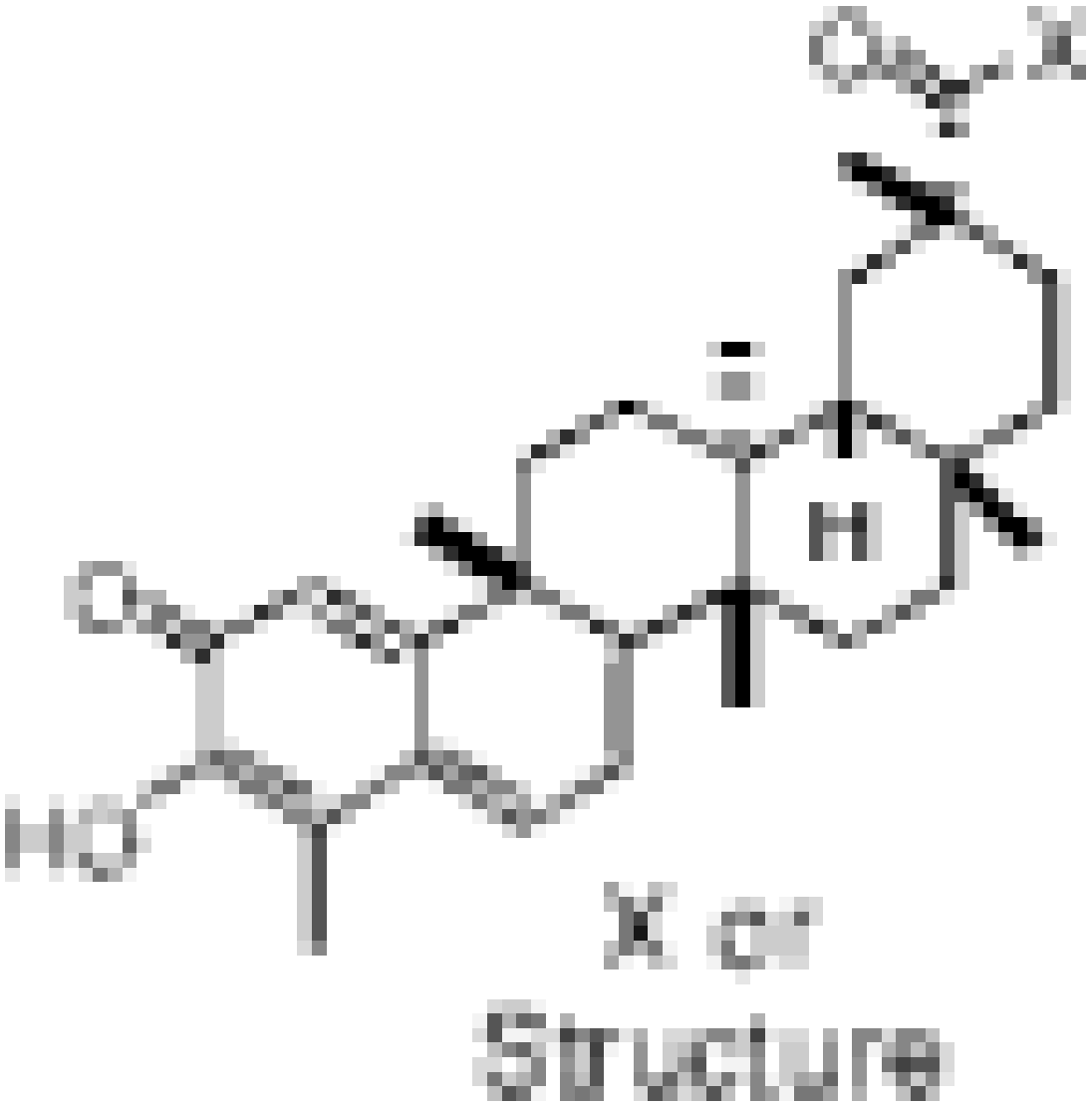	~(

Code	Structure	Activ EC_{50} (I in SW
Pristimerin		<(

Code	Structure	Activ EC_{50} (I in SW
Dihydrocelastrol	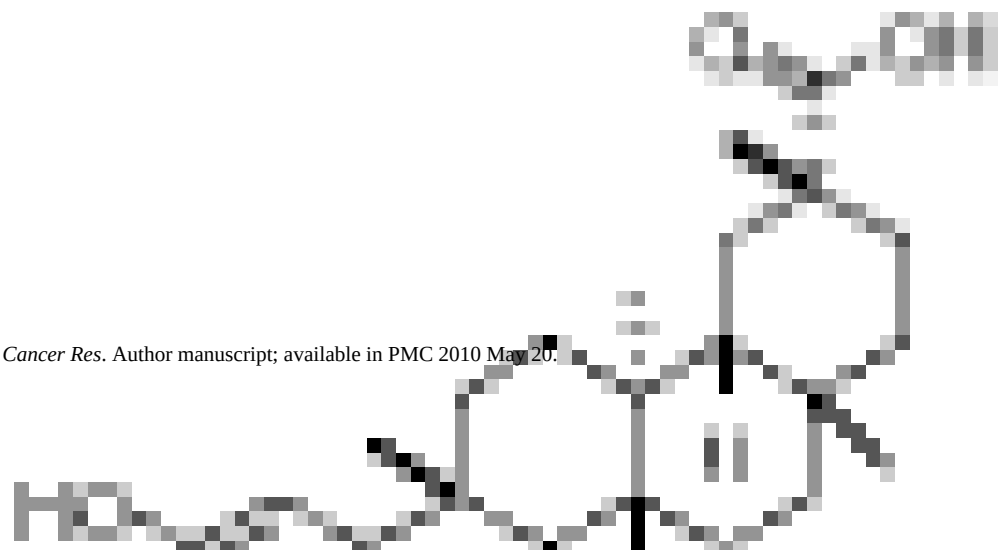	Inac

Code	Structure	Activ EC_{50} (in SW
CA01	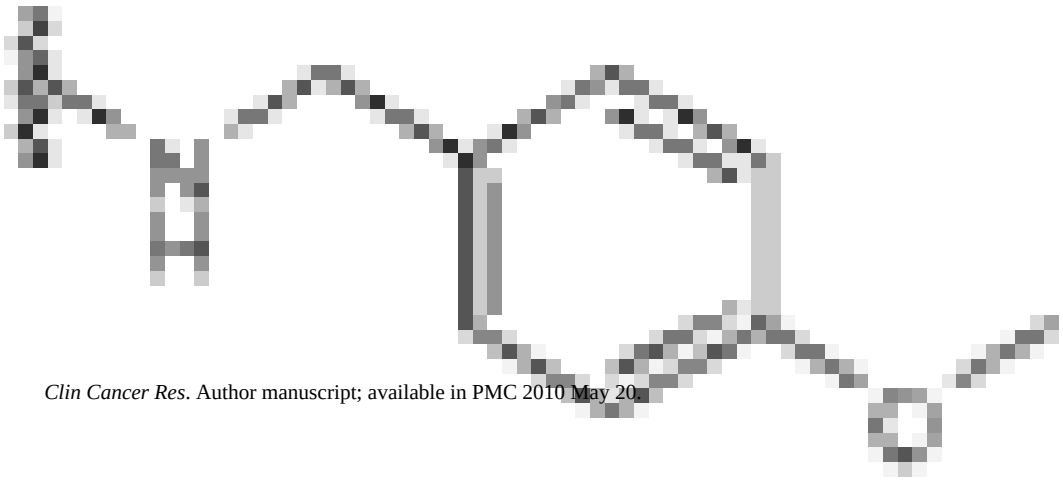	Active

Code	Structure	Activ EC_{50} (I in SW
CA02		Inac

Code	Structure	Activ EC_{50} (I in SW
CA03	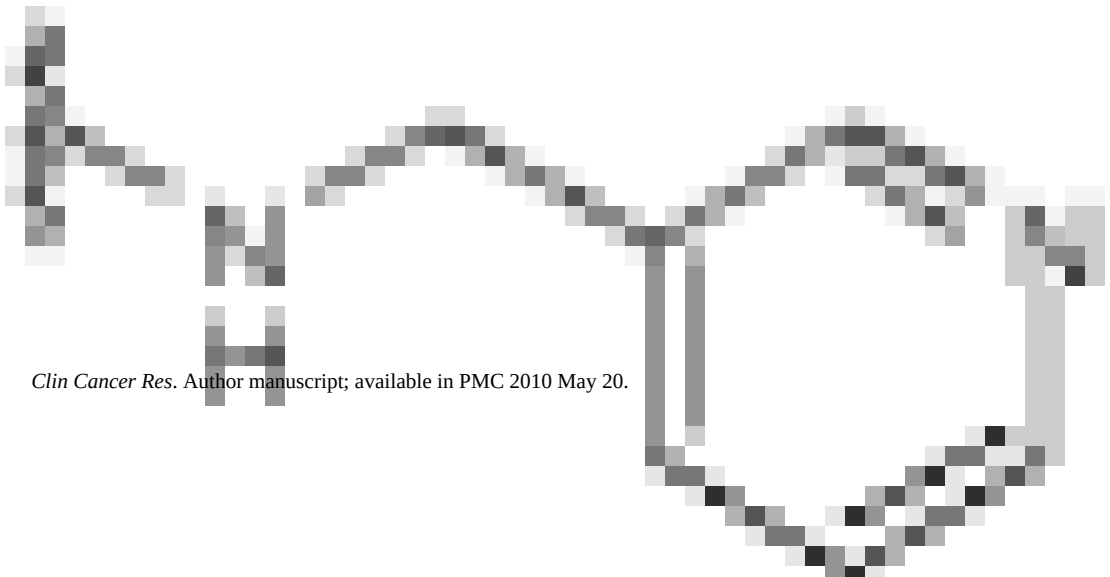	Active

Code	Activ EC_{50} (I in SW
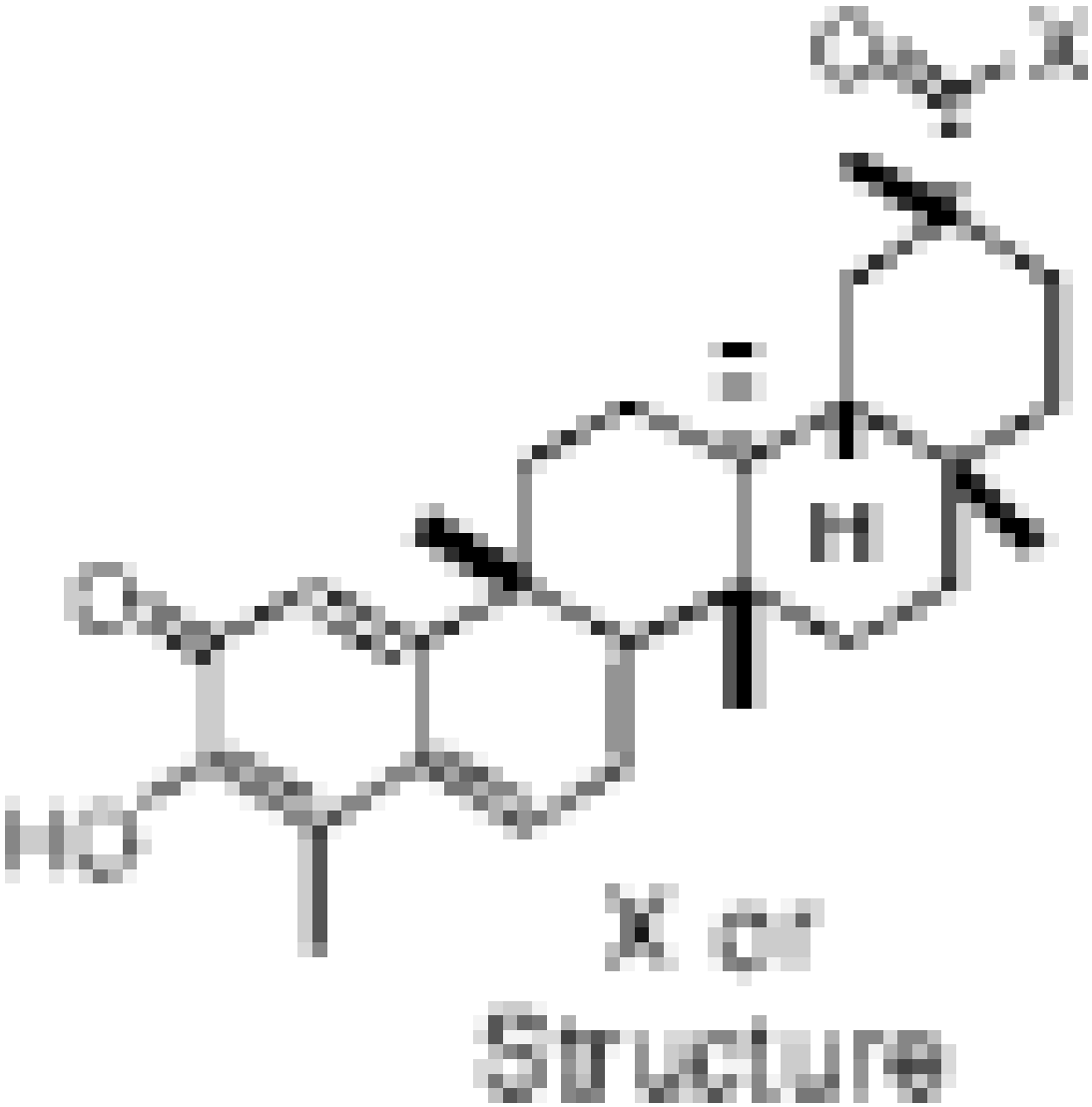	
CA04	Active
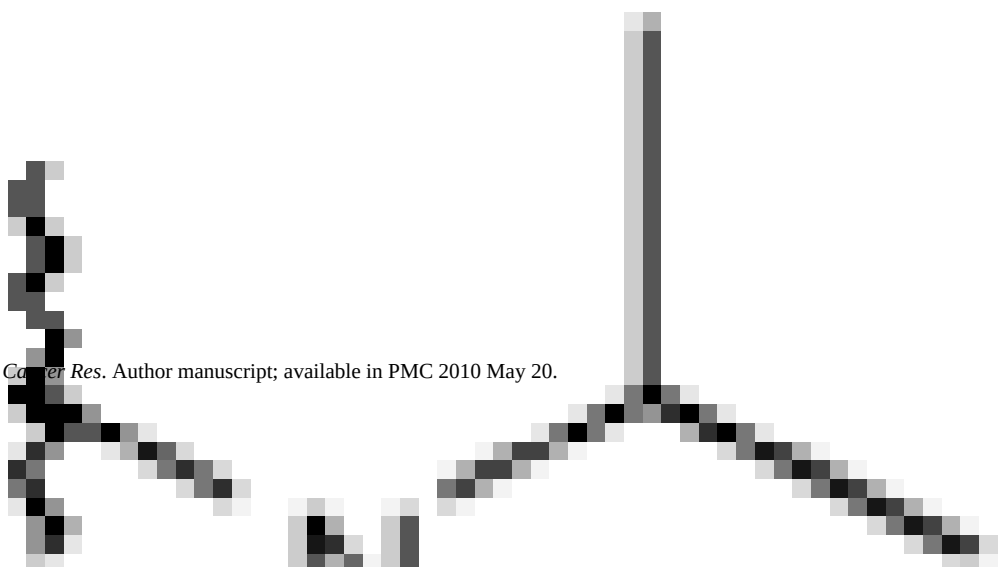	

Code	Structure	Activ EC_{50} (in SW
CA05		Active

Code	Structure	Activ EC_{50} (I in SW
CA06		Active
CA07	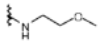	Active
CA08		Inac

Code	Structure	Activ EC_{50} (I in SW
CA13	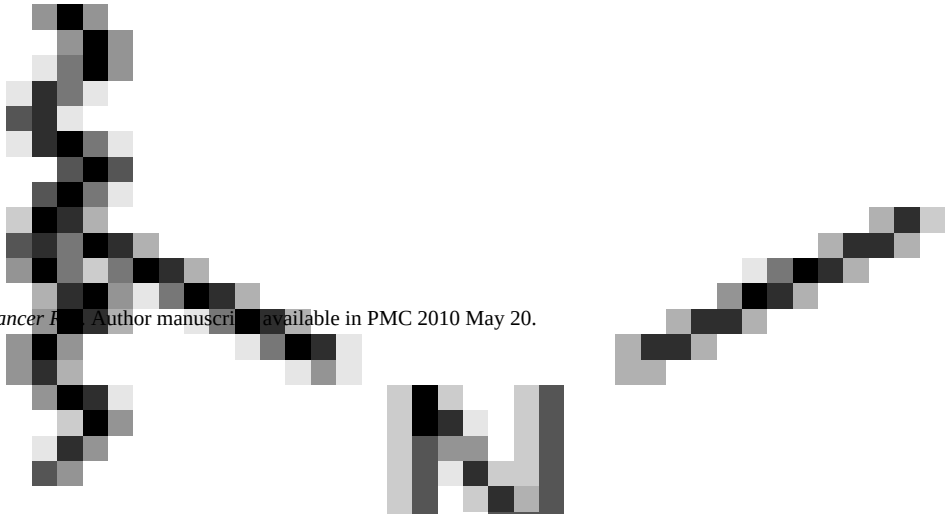	Inac

Code	Activ EC_{50} (I in SW
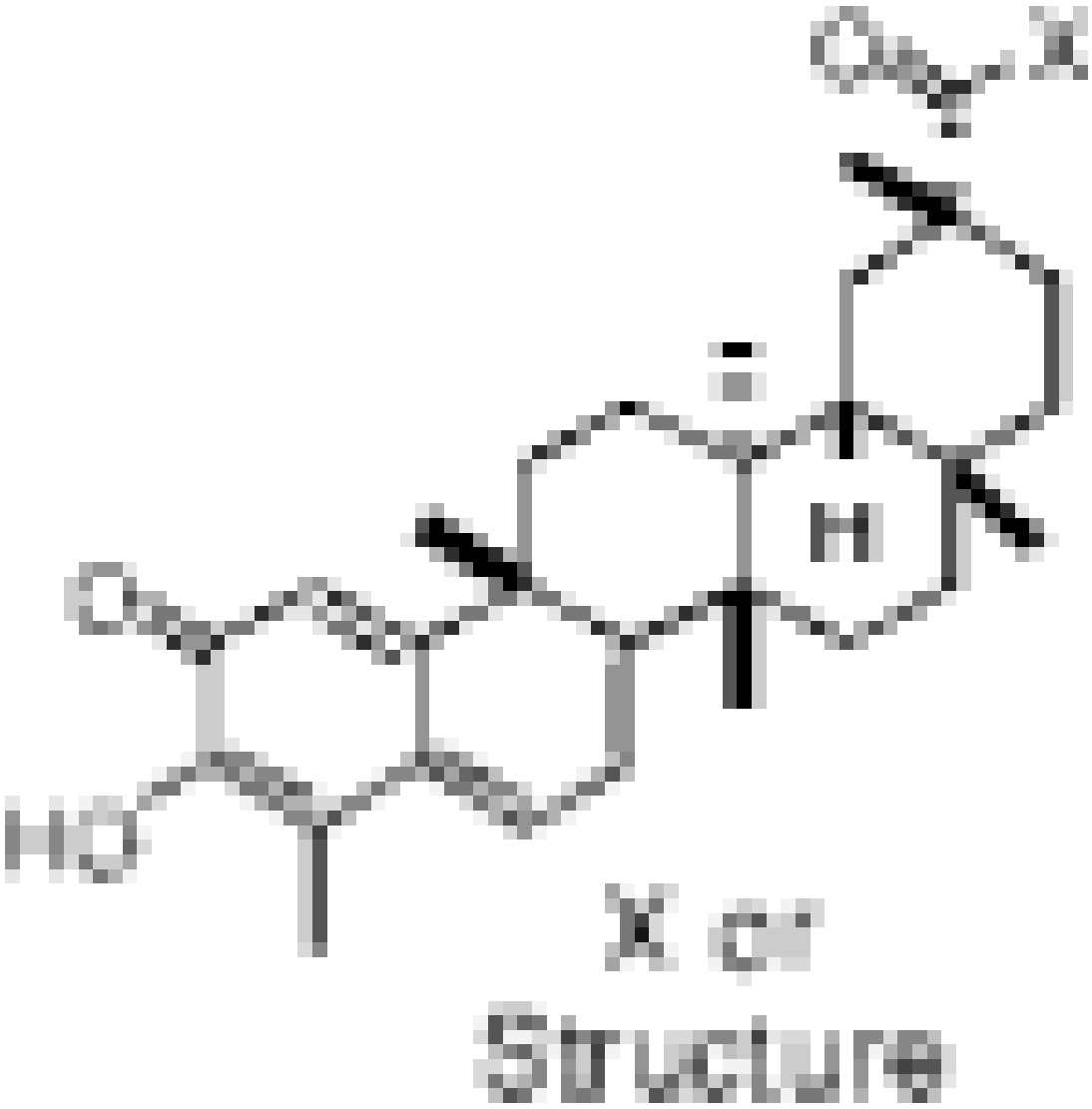	
CA14	Inac
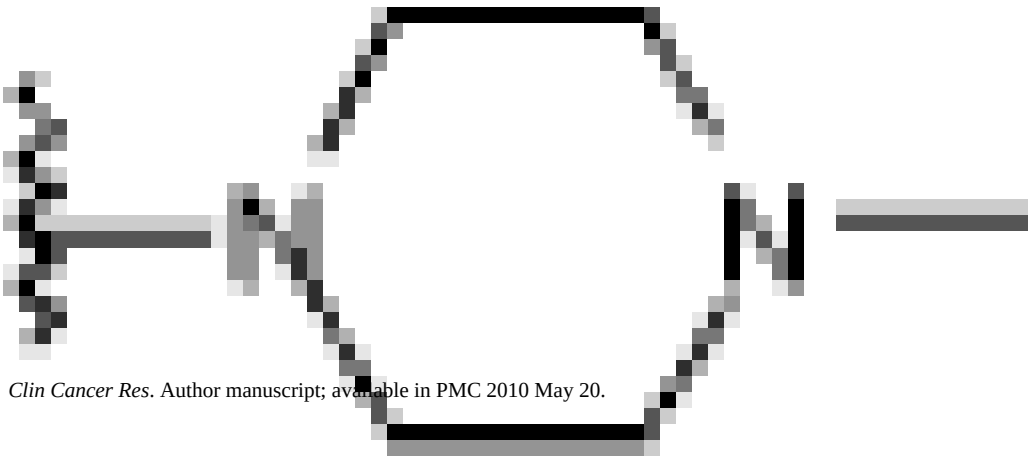	

Code	Structure	Activ EC_{50} (in SW
CA15	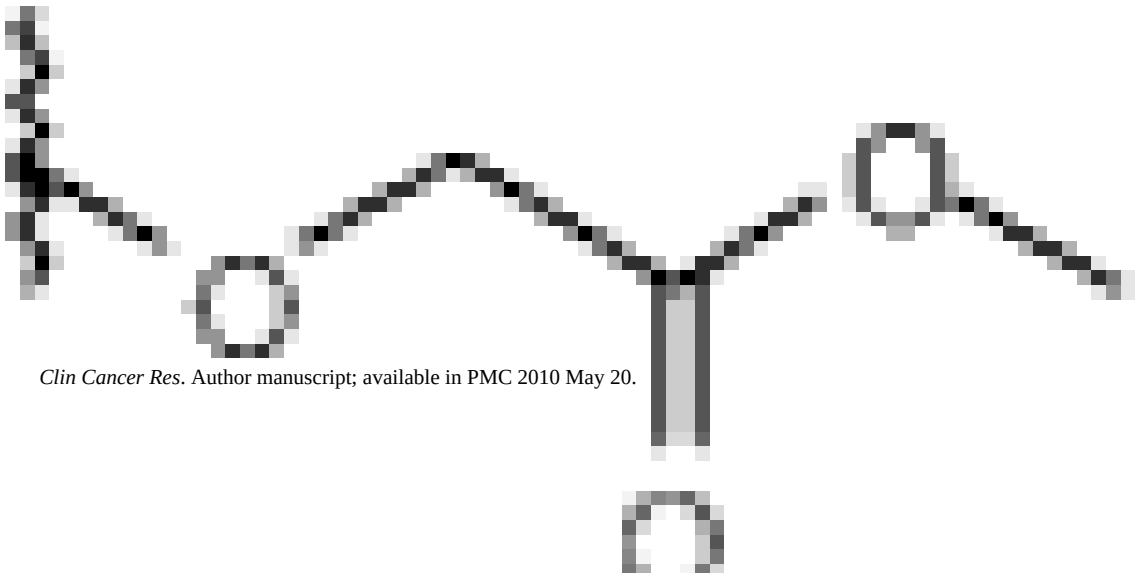	Inac

Code	Structure	Activ EC_{50} (I in SW
CA16		Active
CA18		Active
CA19		Active

NOTE: Active: >50% inhibition of melanoma cell viability. SW1 is a mouse melanoma cell. WM115 and WM793 are human melanoma cells.

Abbreviation: ND, not determined.

* Represent single analysis.